Clays and Clay Minerals, Vol. 43, No. 1, 116–127, 1995.

GEOCHEMISTRY AND MINERALOGY OF A MODERN BUSERITE DEPOSIT FROM A HOT SPRING IN HOKKAIDO, JAPAN

AKIRA USUI[1] AND NAOKI MITA[2]

[1] Department of Marine Geology and
[2] Department of Geochemistry, Geological Survey of Japan
1-1-3 Higashi, Tsukuba, Ibaraki, Japan 305

Abstract—The hot spring water discharging from a flank of an active volcano is precipitating unique monomineralic manganese deposits over volcanic terrain. The major and trace element chemistry, XRD mineralogy, DTA, and SEM observations indicate that the deposits consist of 10 Å phyllomanganate (buserite) accommodating inter-layer Ca and Mg with negligible amounts of detrital minerals. Other metallic elements can be accommodated by buserite, but concentrations are negligible ranging less than 10 ppm to 500 ppm. Abundance and pattern of REE (less than 100 ppm in total) are similar to those from hydrothermal manganese deposits. The buserite is enriched in Ca and Mg but depleted in Na in comparison with those in the spring water. The distribution coefficients for Ca, Mg and Na between the buserite and the host water were calculated assuming an ion-exchange equilibrium in the Yuno-Taki Falls, which proved applicable to other manganese deposits from surficial environments on land and oceans.

Key Words—Buserite, DTA, Hot spring, Ion-exchange equilibrium, Manganese deposit, Phyllomanganate, REE, SEM, Todorokite, Volcano, XRD, Yuno-Taki Falls.

INTRODUCTION

Modern manganese oxide deposits or sinters have been reported in various surficial environments from deep ocean floors to deserts as summarized by Dixon and Skinner (1992). Since manganese is a mobile element in surficial physico-chemical conditions, the dissolved manganese in aqueous solutions, such as hydrothermal waters, ground waters, soil interstitial waters, sea water, etc. is easily precipitated as clay-size oxide particles when oxidizing environments are encountered. Growing large manganese oxide deposits are reported typically near submarine low-temperature hydrothermal vents associated with mid-oceanic spreading centers and submarine island-arc volcanoes (Moore and Vogt 1976, Corliss *et al* 1978, Lonsdale *et al* 1980, Cronan *et al* 1982, Lalou *et al* 1983, Thompson *et al* 1985, Usui *et al* 1986, Alt *et al* 1987, Bolton *et al* 1988, Usui *et al* 1989, Usui and Nishimura 1992). On the other hand, modern subareal active manganese deposits are usually small in size and in deposition rate. For instance, cold spring deposits (Brown 1964, Mustoe 1981), desert varnishes (Potter and Rossman 1979a, Raymond *et al* 1992), stream deposits (Robbins *et al* 1992, Robinson 1993), and disseminated manganese deposits and manganese aggregate in soils (Wada *et al* 1978) have been reported. Subareal manganese oxide material derived from discharging hot spring waters were reported in some Japanese Quaternary volcanos (Hariya 1985, Suzuki and Sakai 1991), and were suggested to form in the final stage of magmatic activity (Yoshimura 1952). However, their geochemical and mineralogical characteristics and the factors controlling compositional variability are not well documented.

The Yuno-Taki Falls manganese deposit, which is possibly the largest known actively-forming deposit of this type on land, was first described by Hariya *et al* (1992). The primary manganese oxide is precipitating in contact with hot waters running over the waterfall. This article focuses on geochemical and mineralogical characterization of the Yuno-Taki manganese oxide deposits precipitating from hot waters discharging on the flank of the active volcano, Mt. Me-Akan in Hokkaido, and on the factors controlling compositional variations in minor element composition among them with reference to host solutions in comparison with other similar deposits. The processes and environments of the precipitating deposits can give us clues to understand ancient and modern manganese oxide deposits on sea floors and on land surfaces.

FIELD SETTING OF MANGANESE DEPOSITS

Mount Me-Akan is an active composite volcano in the Akan volcano group on the volcanic front in Hokkaido Island, Japan (Figure 1). The Yuno-Taki Falls (650 m above sea level) are located on the lower slope of the peak, Akan-Fuji (elevation of summit: 1474 m) in the Akan National Park. The temperature of the rock surface at the summit is 47 to 50°C, and the adjacent peak, Pon-Machineshiri, erupted in 1955 and 1956 (Satoh 1964, Mitani *et al* 1964). Spring water (42–43°C) is discharging at the Yuno-Taki Falls over the front margin of the youngest andesitic lava flow and volcanic ejecta named "Akan-Fuji lava" (Hariya

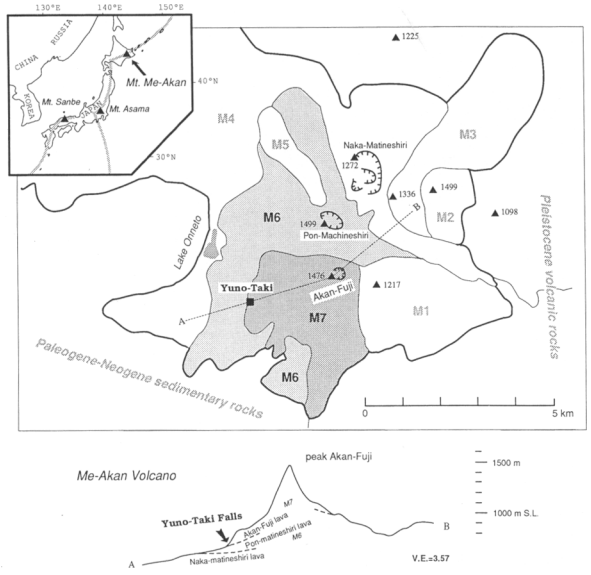

Figure 1. Location and simplified geological map of Me-Akan volcano area and a vertical profile along A to B. Modified from Satoh (1964) and Mitani *et al* (1964). Solid triangles with numbers are volcanic pinnacles and elevations from sea level in meters. M1 to M7 enclosed by a thick line are the Holocene volcanic lavas in descending order of age of eruption. Curved lines with ticks denote margins of craters. The corner insert map shows other similar Mn deposits and the volcanic fronts on island-arc systems around Japan.

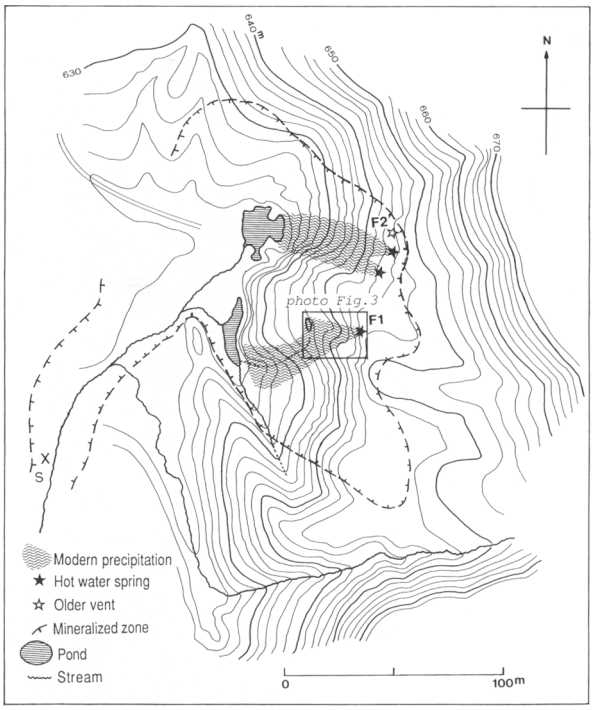

Figure 2. Terrain map of Yuno-Taki Falls, location of vents of spring waters, and areas of manganese mineralization modified from Umemoto *et al* (1956). Hot spring waters are discharging from the flank of Akan-Fuji (to the east) and make up two major waterfalls, F1 and F2, forming modern manganese beds over volcanic rocks. Analyses were carried out on F1 deposits where flow rate is apparently greater.

et al 1992). Figure 1 shows a simplified geological map and profile of the volcano. The hot spring water from the vents falls 30 to 40 meters making up two major waterfalls on the rocky slope of 30 to 40° gradient (Figure 2). The permeable nature of the Akan-Fuji lava may result in effective circulation of meteoric and underground waters. The Akan-Fuji lava is thought to have erupted between 2000 to 800 years B.P. based on ^{14}C dating of ash beds (Yokoyama *et al* 1976). These manganese deposits overlie the andesitic lava, or less frequently, the beds of buff to white calcareous sinters (calcite) several meters thick. There is no positive field evidence of modern precipitation of carbonates on the waterfall. The age of the calcareous sinters is unknown, but may be younger than the Akan-Fuji lava since they cover the lava.

Black manganese deposits up to one meter thick underlie the running water (Figure 3). The bulk of fresh deposits on the waterfalls are semiconsolidated but easily scraped off with a steel knife. Cores up to 20 cm long of earthy black manganese oxide show no apparent sedimentary structure. The deposit is a wad or bog manganese ore. Abundant living algae develop on the surface of the manganese deposits along the paths of the stream. The running water is still precipitating thin manganese deposits, just before it finally merges into a larger river more than 300 meters downstream. Older more consolidated manganese deposits form a matrix cementing volcanic breccia and cobbles more than three meters below the ground surface around this area. The total lateral dimensions of the mineralized area are about 100 × 300 meters (Figure 2). More than 3500 tons of manganese ores were commercially mined until 1954 (Umemoto *et al* 1956).

The water discharging from vents is weakly acidic (pH 6) and lacks dissolved oxygen (Hariya *et al* 1992). The water quickly changes to weakly alkaline (less than pH 8) and becomes oxygen-saturated in the course of falling about 20 meters over the steep rocky wall. The total dissolved manganese in the vent water drops from 3 ppm to 2 ppm while running downstream as a result of the precipitation of manganese oxide. The drop of dissolved Mn content strongly suggests precipitation of manganese in progress. In fact, we recovered newly formed 10 mm films of Mn oxide precipitate from fixed plastic containers after one-year of exposure in the middle of the waterfall (October 1992 to November 1993). However, the measured pH-Eh conditions do not indicate strong oxidation of Mn^{2+} despite being saturated with DO. The oxidation process is possibly accelerated by microbial mediation (Mita *et al*, 1994). Concentrations of Ca^{2+} (95 ppm), Mg^{2+} (115 ppm), Na^{+} (116 ppm), and K^{+} (29 ppm) of the water are

https://doi.org/10.1346/CCMN.1995.0430114 Published online by Cambridge University Press

https://doi.org/10.1346/CCMN.1995.0430114 Published online by Cambridge University Press

constant over the waterfall. More details of water chemistry and a role of bacterial mediation of this deposit will be presented elsewhere by Mita *et al* (1994).

SAMPLES AND ANALYTICAL METHODS

One cm, or less, surface was taken from 30 locations mostly beneath the running water, stored wet in the spring water, and kept less than one week in a refrigerator at 4 to 8°C before analysis. Six cores (10 to 20 cm long) were also collected on the wall of the waterfall. Figure 3 demonstrates sample locations at one (Fall F1) of the two waterfalls. Twenty three samples from surface deposits and 22 samples from three cores (at 2 cm interval) were analyzed.

The wet samples were rinsed and ground with distilled water in an agate mortar, followed by X-ray powder diffraction (XRD) analysis while wet at a room temperature. The air-dried and 110°C-dried powders were also subjected to XRD in order to examine mineralogical change during dehydration. Aliquots (0.5–1 gram) of air-dried powders were analyzed by Multi-element ICP spectroscopy for 35 elements. We used $HF/HNO_3/HClO_4$ mixed acid for digestion. The Chester extraction method (Chester and Hughes 1976) was not necessarily used because of negligible amounts of insoluble fraction in the deposits. The analyses were done by X-ray Laboratories Co. Ltd., Canada using Multi-channel Type ARL3560 ICP-AES. Rare earths were determined by ICP mass spectrometer by the same laboratory calibrated with reference sample SY-2 (Govindaraju 1989). Carbon (organic form and carbonate form) and sulfur (free sulfur plus sulfide form and sulfate form) were calculated by C-S analysis with Horiba Type HF-500/EMIA-250 at the Geological Survey of Japan (GSJ), assuming that thermal treatment at 450°C for 12 hours releases organic C, free and sulfide S (Krom and Berner 1983). Contents of free sulfur including sulfide were below detection limit (0.01 wt. %) in all samples. Reliability of each analysis of elements was checked with USGS Rock Standard Nod-P-1 and Nod-A-1 (Flanagan and Gotterfried 1980) and other reference manganese samples at GSJ (cross-checked with atomic absorption spectroscopy and instrumental neutron activation analysis). The maximum analytical errors are in the range of 5–10 relative % for major elements and 5–20% for minor and trace elements. The water content is the weight loss after heating at 110°C for 12 hours in an oven. Selected air-dried samples were observed and analyzed by scanning electron microscope (SEM) and energy-dispersive X-ray analysis (EDX). Differential thermal analysis (DTA) was carried out for two typical samples.

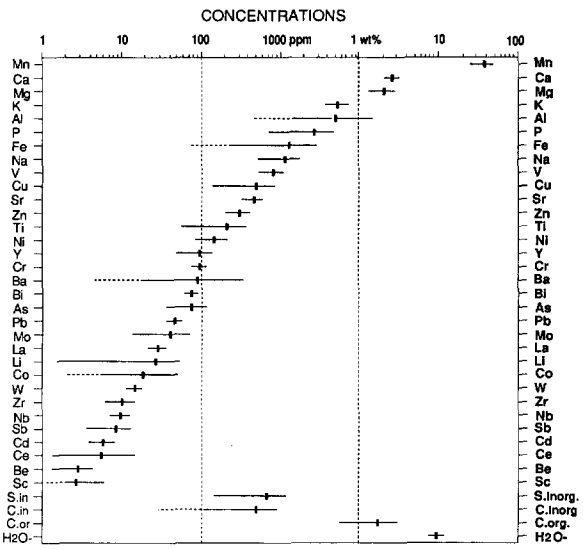

Figure 4. Average ± one standard deviation of concentrations of 23 elements in decreasing order in the Yuno-Taki deposits (sample no.: 50).

Chemical and mineralogical characteristics of manganese deposits

Major and minor element chemistry. Among 40 elements analyzed, the average concentrations of Mn, Ca, Mg, and organic C exceed 1 wt. %, those of K, Al, P, Fe, Na exceed 0.1 wt. %, but other elements (inorganic C, total S, V, Cu, Sr, Zn, Ti, Ni, Y, Cr, Ba, Bi, As, Pb, Mo, REEs, Li, Co, W, Zr, Nb, Sb, Cd, Sc, and Ag; in descending order) are less than 0.1 wt. %, as shown in Figure 4. From the field observations, most of the surface samples taken below running water contain living algae and fragments of plants which yield high organic carbon contents (up to 5 wt. %; average of 1.7 wt. %). The variations of major and minor elements are small throughout 50 samples from surface and cores of the Yuno-Taki deposits. We observe no significant compositional variations in major and minor elements with distance from the vent of waterfall F1 to about 50 m downstream or no clear downcore variations (Table 1). The only important downcore variation in chemical composition is abrupt depletion of organic carbon by a factor of six or more at depths of 2 to 6 cm below the surface in the three cores. The decrease of organic carbon may be caused by decomposition of organic

←

Figure 3. View of the Yuno-Taki Fall F1 and sample locations of manganese deposits in Table 1 only. Alphabetical labels are locations of core samples up to 20 cm depth. Mn-mineralized zone is enclosed with dotted lines. Hot waters are flowing over the vent. Distances (10 m, 20 m) are measured from the vent (marked 0 m). Some part of surface is covered with green moss plants.

Table 1. Atomic ratios of (Ca + Mg)/Mn and Mg/(Ca + Mg), showing no significant downcore or downstream variation over the fall. Atomic ratios were calibrated assuming some parts of Ca and Mg are accommodated as carbonate or sulfate. The reciprocal of the ratio falls mostly within the range between 5.7 to 7.1 close to 6.0 for the ideal buserite. Sample numbers are the same as in Figure 3.

Downstream variation				Downcore variation			
Site	Distance from vent (m)	(Ca + Mg)/Mn atom. ratio	Ca/(Ca + Mg) atom. %	Core	Depth from surface (cm)	(Ca + Mg)/Mn atom. ratio	Ca/(Ca + Mg) atom. %
F1-#1	0	0.154	46.9	A	0–2	0.140	44.7
F1-#2	5	0.162	52.0		2–4	0.139	47.7
Core A	7	0.140	44.7		4–6	0.151	50.4
F1-#4	8	0.150	57.0		6–8	0.157	47.9
F1-#3	10	0.152	43.8		10–12	0.174	46.0
F1-#5	11.5	0.162	67.8	C	4–6	0.171	47.6
F1-#8	14	0.166	44.1		8–10	0.171	47.7
F1-#7	14	0.172	42.2		10–12	0.181	47.0
F1-#6	14.5	0.174	51.3		12–14	0.174	46.8
F1-#9	19	0.173	60.2	E	0–2	0.149	56.0
S-#4	200	0.147	47.2		2–4	0.141	49.7
S-#9	200	0.152	47.5		4–6	0.165	43.4
					6–8	0.193	41.2
					8–10	0.182	43.4
					12–14	0.187	43.8
					16–18	0.158	45.5
					18–19	0.184	45.0
Ave. & S.D.		0.159 ± 0.011	50.1 ± 7.7			0.166 ± 0.017	46.7 ± 3.4

material in the deeper part of the deposits after burial. The process may cause mildly-reduced conditions in the depth.

Correlation and cluster analyses were done on 42 selected surface and core samples (more than 40 wt. % Mn and less than 1 wt. % Al) for 17 abundant elements (Table 2, Figure 5). As shown in the dendrogram, the 17 elements are fairly well grouped into four categories: 1) Mn, Ca, Mg, K, Cu, Ni, Zn, and V in a manganese mineral, 2) Al, Fe, and Na in detrital silicate minerals, 3) carbon and P in organic materials, 4) Ba, Sr, and S possibly as sulfate minerals. The total, Mn, Ca, Mg, water, and organic C, amounts to 75% to 98% by weight assuming stoichiometric oxides MnO_2, CaO, MgO, H_2O, and cellulose CH_2O in algae.

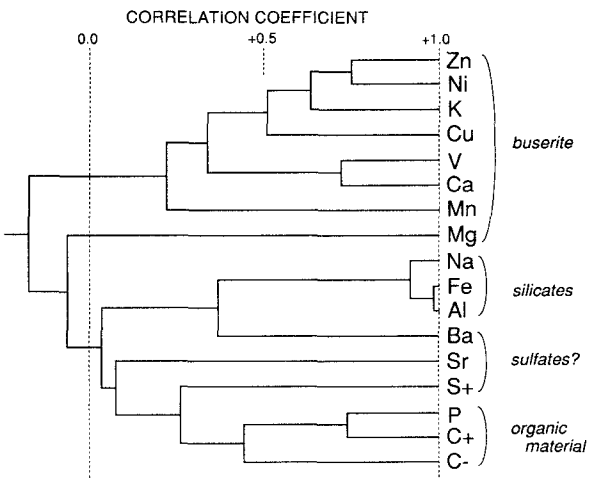

Figure 5. Results of cluster analysis for major and minor elements in surface deposits (n = 22). A possible grouping demonstrates four different components. C+ means residual fraction at 450°C, and C− means the released fraction below 450°C.

Mineral composition. SEM observations reveal dominant clay-sized (several μm across and less than 0.1 μm thick) crystals of a manganese oxide mineral in all samples. The estimated mean dimension of the manganese mineral from the broadening of basal 10 Å peak on powder XRD patterns ranges 90 to 100 Å according to Scherrer equation (Klug and Alexander 1954). The actual size (thickness) of the thin crystals may be larger since the equation assumes uniform stacking. The estimated sizes from XRD broadening and SEM observation are fairly in good agreement.

The manganese oxide crystals have blade- or plate-like habit, which form knobby columns or bumpy aggregates (Figures 6A and 6B). The surface of knobs and aggregates commonly show boxwork features of thin crystals. The boxwork feature is observed in the depth of core samples as well as surfaces. The crystals often encrust long tubes of algae (Figures 6C and 6D). This structure is observed only in surface samples. The manganese mineral very rarely grows inside the algae but usually surrounds its tubes as several μm thick encrustation. The size, blade-like habit and boxwork feature of the manganese deposits are common to manganese sinters from a cold spring water in Washington, U.S.A. (Mustoe 1981) and submarine hydrothermal manganese deposits (Usui *et al* 1989). Small amounts of diatom tests, and more rarely, silicate particles are

https://doi.org/10.1346/CCMN.1995.0430114 Published online by Cambridge University Press

Table 2. Correlation matrix for chemical composition of manganese deposits of the Yuno-Taki Falls F1 (n = 42).

	C−	C+	P	S+	Sr	Ba	Al	Fe	Na	Mg	Mn	Ca	V	Cu	K	Ni
C+	0.466	1.000														
P	0.418	0.743	1.000													
S+	0.207	0.371	0.245	1.000												
Sr	−0.098	0.295	0.491	0.010	1.000											
Ba	−0.122	0.016	−0.009	0.115	0.034	1.000										
Al	0.210	0.092	0.009	0.101	−0.104	0.437	1.000									
Fe	0.212	0.096	0.016	0.102	−0.087	0.446	0.988	1.000								
Na	0.190	0.202	0.159	0.090	0.077	0.290	0.929	0.908	1.000							
Mg	0.099	−0.117	−0.312	0.042	−0.104	−0.034	−0.051	−0.042	−0.168	1.000						
Mn	−0.106	−0.205	0.084	−0.082	−0.081	0.012	−0.205	−0.193	−0.191	−0.395	1.000					
Ca	0.163	−0.338	−0.034	−0.159	−0.232	−0.084	0.126	0.160	−0.040	−0.282	0.342	1.000				
V	−0.086	−0.368	−0.078	−0.278	−0.019	−0.190	−0.227	−0.206	−0.291	−0.368	0.234	0.730	1.000			
Cu	−0.165	−0.221	0.006	0.019	−0.017	0.465	0.297	0.301	0.226	0.035	0.104	0.219	0.142	1.000		
K	−0.475	−0.679	−0.447	−0.328	−0.048	0.059	0.107	0.106	0.055	−0.284	0.254	0.510	0.682	0.404	1.000	
Ni	−0.517	−0.644	−0.510	−0.318	−0.084	0.010	−0.154	−0.141	−0.232	0.157	0.232	0.219	0.408	0.552	0.717	1.000
Zn	−0.153	−0.416	−0.165	−0.221	0.151	−0.031	−0.039	0.005	−0.105	0.228	0.028	0.403	0.498	0.668	0.560	0.752

Note: Subscript (+) means carbonate or sulfate; (−) organic.

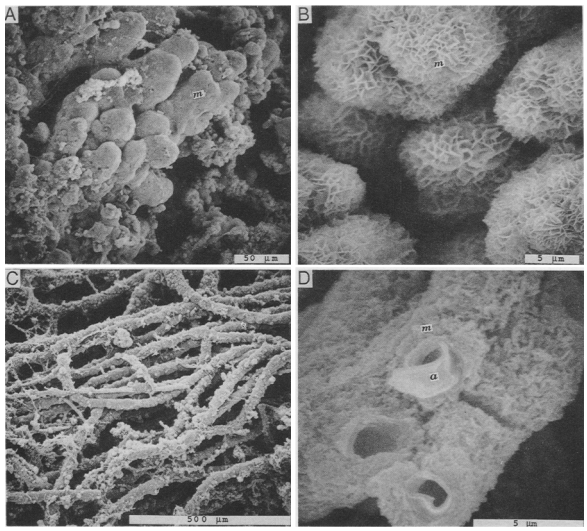

Figure 6. Scanning electron photomicrographs of manganese precipitates in surface deposit F1-#7. "m" and "a" denote buserite and algae, respectively. A: common feature of knobby and columnar growth structures of buserite. Surface as well as interior is composed of buserite crystals. B: close-up of surface of knobs. C: tubes of algae entirely coated by buserite. D: close-up of broken surface of algae showing empty tubes thickly coated with buserite crystals. Precipitates grow only outside the tubes not inside.

associated with manganese deposits. Traces of clay minerals and plagioclase were detected in a few samples by XRD.

Based on previous mineralogical studies of manganese minerals from supergene and low-temperature hydrothermal deposits, together with synthesis experiments, the initial manganese oxide phases from Mn^{2+}-bearing alkaline oxidizing aqueous solutions are 10 Å manganate material (Buser *et al* 1954, McKenzie 1971, Giovanoli 1980, Potter and Rossman 1979b, Usui *et al* 1989). The 10 Å manganate material is subdivided into a phyllomanganate, buserite, and a tunnel-structure mineral, todorokite (Burns *et al* 1983, Chukhrov *et al* 1985).

Buserite is characteristic of an expandable and contractible sheet, and accommodates hydrated stabilizing interlayer cations (Paterson *et al* 1986b, Golden *et al* 1986, Post 1992). One of the important chemical characteristics of buserite is that the exchangeable interlayer cations (Ca^{2+}, Mg^{2+}, Cu^{2+}, Ni^{2+}, Co^{2+}, and $2Na^{+}$) occupy specific structural sites and thus the atomic ratio of total metals to Mn is constant 1:6 (Usui 1979, Chukhurov *et al* 1985) or 1:7 (Golden *et al* 1986). The 10 Å spacing can contract to 7 Å on dehydration at a room temperature. It can expand when soaked with dodecylammonium ion to 25 Å spacing (Paterson *et al* 1986a, Arrhenius and Tsai 1981). On the other hand, todorokite has a large tunnel structure with [MnO_6] octahedrons (3 × N; tunnel dimension N ≥ 3) (Chu-

https://doi.org/10.1346/CCMN.1995.0430114 Published online by Cambridge University Press

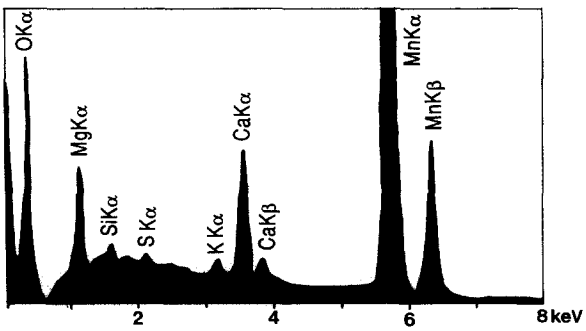

Figure 7. Typical results of EDX analysis of buserite crystals on SEM micrograph (same type as in Figure 6B). Several analyses over several similar samples reveal no significant differences in composition.

khrov *et al* 1985, Turner *et al* 1982, Miura and Hariya 1984, Giovanoli 1985, Post and Bish 1988). Todorokite has no contractible or expandable nature on heating at 100°C (Usui *et al* 1989) or usually up to 400°C (Miura and Hariya 1984, Bish and Post 1989). Thus the criteria for discriminating the two series are: 1) expansion test by dodecylammonium treatment and 2) contraction test to 7 Å by heating at 110°C in air. The second criteria seems more reliable because some synthetic and natural buserites never expand after dodecylammonium treatment for more than one month.

All of the samples taken from the bottom of running water on the Yuno-Taki Falls are typical 10 Å manganate material on XRD pattern when wet and dry at room temperature. However, the samples from dry surface soil 4 m away from the running water and from older outcrops often show a 7 Å reflection probably due to post-depositional dehydration. The 10 Å reflection of all samples disappears and 7 Å appears when dried at 100°C in air. This behavior is common to natural and synthetic buserites. Typical XRD patterns are shown in Figure 8. No significant downstream differences in mineralogical characteristics were observed.

One significant downcore change in mineralogical character is an increase of contractible 10 Å manganate (in air) near the bottom of the core in association with the depletion of organic carbon. The most probable explanation is the existence of divalent Mn as interlayer cations in the buserite, which cannot stabilize 10 Å spacing in air (Usui 1979).

Treatment by dodecylammonium-hydrochloride on some Yuno-Taki deposits also supports the evidence of sheet-structure buserite, showing apparent expansion of basal reflections from 10 Å to 25 Å immediately after soaking in dodecylammonium solution (Figure 8). Another evidence for buserite in the samples is a nearly stoichiometric chemical composition. The calculation of atomic ratios of interlayer cations to Mn (Table 1) shows that the ratio is approximately 1:6

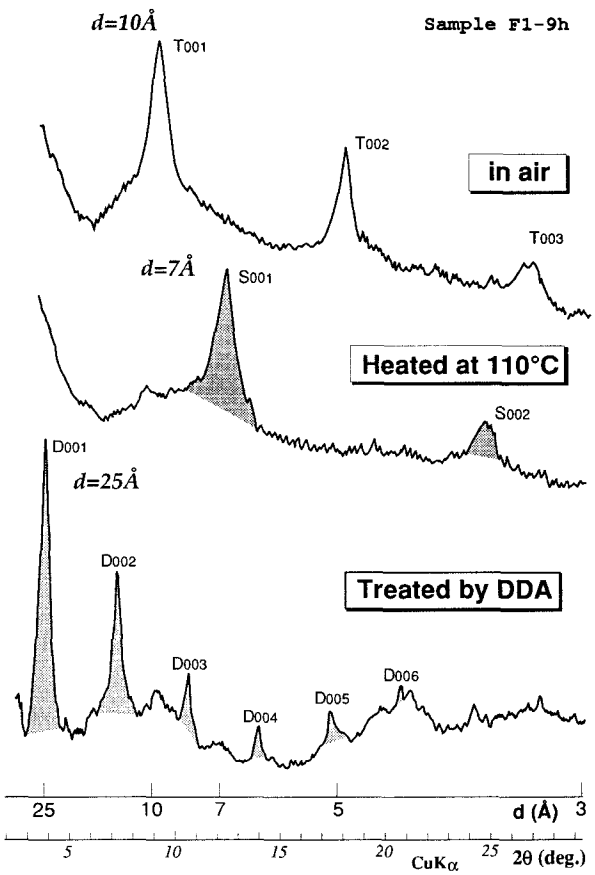

Figure 8. XRD patterns of the wet manganese deposits, a sample heated at 110°C for 2 hours, and a sample treated by dodecylammonium (DDA) solution at room temperature. Note the contraction of 10 Å basal reflections to 7 Å and the expansion to 25 Å, both indicating sheet structure of buserite.

(0.163 ± 0.015) which is close to the ideal ratio of synthetic buserite (Usui 1979, Giovanoli and Brütsch 1979). EDX analyses again indicate that the crystals are composed mainly of Mn, Ca, Mg and O (Figure 7). The Ca and Mg accommodated by the buserite was calculated by subtracting the part as carbonate and sulfate which was substantially negligible. The total concentrations of other possible interlayer divalent cations (Cu, Ni, Zn, and Co) are also negligible (less than 0.003 atom. % to Mn) for all the samples. This calculation shows that Ca and Mg are accommodated as (Ca, Mg)-buserite which is isomorphic with natural and synthetic buserites. The probable formula of the buserite is $(Ca_{0.5}, Mg_{0.5})O \cdot 6MnO_2 \cdot nH_2O$.

DTA curves for two Yuno-Taki samples show close similarity to those of marine buserites which have two endothermic peaks at around 100°C and 200–250°C (Figure 9) most probably due to loss of interlayer waters as suggested by Potter and Rossman (1979b). By contrast, tunnel-structure todorokites show no substantial

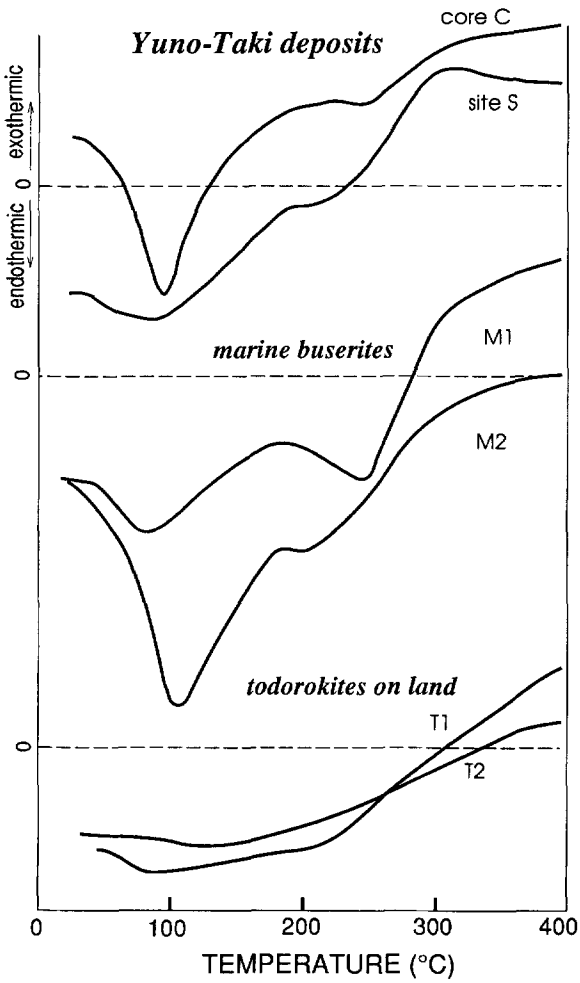

Figure 9. DTA curves for two samples from Core C in comparison with 10 Å manganates from land (todorokites from the Tertiary hydrothermal deposits: T1, Todoroki mine and T2, Ikeshiro mine) and ocean (marine buserites: M1, hydrothermal deposits from the Bonin arc seamount and M2, Mn nodule buserite from the Central Pacific Basin). Note two typical endothermic peaks (90–110°C and 200–250°C) for buserites due to dehydration of interlayer waters in contrast to no peak for todorokite.

peaks indicating gradual dehydration like zeolitic waters. This is consistent with the results of thermal treatment of todorokite by Bish and Post (1989). It is thus concluded that the Yuno-Taki deposit is a unique monomineralic (Ca, Mg)-buserite deposit having nearly stoichiometric chemical composition.

REE patterns. The rare earth element (REE) pattern and abundance of two Yuno-Taki deposits are generally similar to those from hydrothermal manganese deposits from land and oceans. The total contents of REEs (La to Lu) of the deposits range 18 to 27 ppm with a maximum of 6.8 ppm La. The total REE is within the range of reported marine hydrothermal

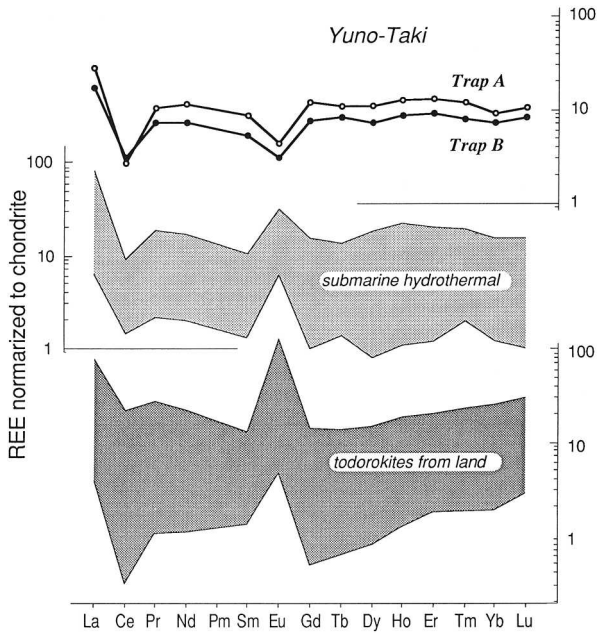

Figure 10. REE patterns of manganese samples of newly precipitated samples in the Yuno-Taki during 1992 to 1993 (Traps A and B from Points 3 and 4 in Figure 3) in comparison with those of hydrothermal 10 Å manganates from land (three todorokite samples as in Figure 9) and ocean (five marine hydrothermal Mn deposits from the Bonin arc seamounts). The abundances are normalized to averaged chondrites by Evanson *et al* (1978).

manganese deposits (Hein *et al* 1987). The common Ce negative anomaly suggests that all the three types were formed from reducing to suboxic solutions in contrast to the positive anomaly observed in hydrogenetic manganese minerals formed from oxygenated normal sea water (Glasby *et al* 1987, Kunzendorf *et al* 1993). Figure 10 demonstrates a significant relative negative Eu anomaly of the Yuno-Taki deposits. The Eu positive anomaly in hydrothermal deposits, in general, reflects interaction of heated waters with substrate volcanic rocks of high Eu content during circulation. The characteristic negative Eu anomaly of Yuno-Taki deposits, in contrast, suggests insufficient interaction of ground water with substrate volcanic rocks probably due to low temperature.

Ion-exchange equilibrium of manganese mineral with host solution

When the Yuno-Taki deposits are compared with various submarine hydrothermal deposits and other similar hot spring deposits (Sanbe and Asama), Ca and Mg are enriched and Na, Ba and Mo are depleted. The ternary plots of major elements, Mg-Ca-Na atomic ratio in manganese deposits, demonstrate that each type falls within a narrow specific region (Figure 11, Table 3).

https://doi.org/10.1346/CCMN.1995.0430114 Published online by Cambridge University Press

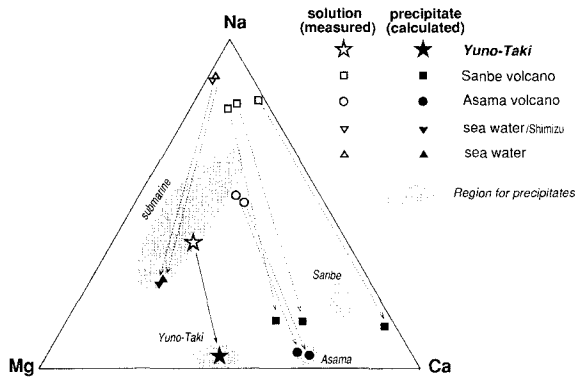

Figure 11. Ternary plots of Mg-Ca-Na for manganese deposits of Yuno-Taki fall F1 and other surface environments. The data source is the same as in Table 3. Sanbe and Asama (Figure 1) yield similar but small Mn deposits. Each group falls in a specific small region. The predicted compositions of buserites (calculated from compositions of host-solution), assuming ion-exchange equilibrium in the Yuno-Taki Falls, well agree with the analyses of natural samples. A relatively variable composition for submarine deposits may be due to larger variety of composition of host fluids and/or mineralogy.

Here we attempt to demonstrate how the composition of minor essential cations (Ca, Mg, and Na) in buserite is controlled by the composition of the host solutions. Assuming that the uniform composition of buserite of the Yuno-Taki deposits is in equilibrium with that of the coexisting hot spring waters, the ratios of distribution coefficients K between elements are expressed as follows.

$$K_{Ca}:K_{Mg} = \frac{[Ca/Mn]_{buserite}}{[Ca/Mn]_{solution}} : \frac{[Mg/Mn]_{buserite}}{[Mg/Mn]_{solution}}.$$

Similarly, this formula can be applied to three elements or more as follows:

$$\frac{[Ca/Mn]_{buserite}}{[Ca/Mn]_{solution}} : \frac{[Mg/Mn]_{buserite}}{[Mg/Mn]_{solution}} : \frac{[Na/Mn]_{buserite}}{[Na/Mn]_{solution}}$$

$$= K_{Ca}:K_{Mg}:K_{Na} = 31.8:17.9:1.00.$$

The calculated Ks indicate relative preference of incorporation of interlayer cations into the buserite sheet. The order of preference, Ca > Mg > Na in the Yuno-Taki deposit, is in accordance with the results of synthesis experiments of buserite, Ni ≫ Cu > Zn ≫ Ca > Mg > Na (Giovanoli and Brütch 1979, Crane 1981). If these factors do not vary significantly within the range of variation of temperatures of each solution, the estimated ratios of these elements in the buserites can be applied to other buserite deposits. The ternary diagram (Figure 11) shows the composition of natural manganates, modern and old, compositions of modern ambient waters, and the expected composition of buserite after calculation on the assumption of equilibrium at Yuno-Taki. The effect of temperature may be negligible in the range of this discussion, because the composition of buserite from an active hydrothermal mound in the Okinawa Trough (Kimura *et al* 1988) also falls in the same region of other submarine deposits in the diagram despite an elevated temperature of 40°C for the hydrothermal vent water. The compositions of the Yuno-Taki deposit, other smaller spring-water deposits (possibly modern), and submarine hydrothermal deposits fall into typical regions in the Na-Ca-Mg diagram of Figure 11. As shown in Table 3, the ratio Ca:Mg:Na in solution is quite variable among these types.

The combined plots on the diagram show a nice coincidence of the buserite composition with those predicted from the K values in the Yuno-Taki deposits. This agreement supports the idea that the minor elements in buserite are in equilibrium and primarily controlled by the chemical composition of the solution. This, in turn, suggests the possibility of estimating the

Table 3. Concentrations of Ca, Mg, and Na in host solutions and buserite deposits from various environments.

	Ca (mg/liter)	Mg (mg/liter)	Na (mg/liter)	pH	Temperature (°C)	Source
Solution						
1) Yuno-Taki Spring	95	115	116	7.1–7.7	42–43	Mita *et al* (1994)
2) Sanbe Spring	135	55	519	5.6–6.0	39	Suzuki and Sakai (1991)
3) Asama Spring	62	32	78	7.7	25	Sakai (personal communication, 1985)
4) Sea water	410	1287	10,685	7.9	4	Gross (1987)
5) Sea water (pumped at Shimuzu)	399	1290	9860	7.8	19	Sato (1991) and Takematsu *et al* (1988)
	(wt. %)	(wt. %)	(wt. %)		No. of data	
Buserite						
1) Yuno-Taki Spring	2.81	1.92	0.10	—	n = 34	this study
2) Sanbe Spring	0.03	0.08	0.12	—	n = 2	this study
3) Asama Spring	3.87	0.93	0.13	—	n = 2	this study
4) Submarine (Bonin)	0.93	2.16	0.17	—	n = 45	this study
5) Sea water (pumped at Shimuzu)	2.00	1.60	0.80	—	n = 1	this study

https://doi.org/10.1346/CCMN.1995.0430114 Published online by Cambridge University Press

composition of original solution from the composition of buserite, whether it is modern or ancient. For instance the Ca/Mg/Na ratio of buserites would indicate relative influences from normal sea water or hydrothermal waters. However, the relative scatter of points for submarine hydrothermal deposits in the diagram suggests partial controls by different mineral composition (for instance, dominant todorokite), by significant contamination of detrital fine particles in the samples, and possibly by fluids with distinctly different composition.

SUMMARY

The Yuno-Taki Falls is precipitating a unique monomineralic manganese deposit from a discharging hot spring. The expandable and contractible features of 10 Å spacing and stoichiometric composition indicate that the deposits are composed of pure (Ca, Mg)-buserite (sheet manganate). The content of other metallic elements are negligible in buserite. There is no significant downstream or downcore variation in chemical and mineralogical compositions over the area of mineralization, though the deposits include small amounts of silicates, organic matter, and possibly sulfate. The typical REE pattern suggests that the host waters did not strongly interact with substrate volcanic rocks.

Distribution coefficients for Ca, Mg, and Na between buserite and spring water were calculated assuming ion-exchange equilibria in the Yuno-Taki deposits and discharging waters. The evidence of preferential incorporation of divalent cations (Ca, Mg) to Na agrees with reported synthetic experiments of buserites. The comparison of the variable composition in buserites from other deposits with their host solutions strongly supports the idea of ion-exchange equilibrium of the three elements between buserite and solution. This, in turn, may be useful in estimating the solution chemistry from the composition of the buserite deposits.

ACKNOWLEDGMENTS

We thank Professor Yu Hariya, Professor G. Arrhenius, and Dr. H. Miura, for their fruitful discussion and comments. Drs. R. E. Ferrell, Jr., H. C. W. Skinner, J. B. Dixon, and B. R. Bolton critically read this manuscript. We are grateful to Drs. K. Tsukimura, S. Terashima, H. Kamioka and M. Ujiie at GSJ for suggestion and help during this study. Dr. Y. Sato of the Tokai University and Ms. Y. Sakai of the Gumma Inst. Public Health are acknowledged for citing their unpublished water chemistry data of the pumped water of the Marine Science Museum at Shimizu, and those at Mt. Asama hot spring. Dr. H. Sawamura is acknowledged for his help during our field survey. Field survey and sampling in the Yuno-Taki Falls were carried out under the official permission of the Ministry of Environment of Japan.

REFERENCES

Alt, J. C., P. Lonsdale, R. Haymon, and K. Muehlenbachs. 1987. Hydrothermal sulfide and oxide deposits on seamounts near 21°N, East Pacific Rise. *Geol. Soc. Amer. Bull.* **98**: 157–168.

Arrhenius, G., and A. G. Tsai. 1981. Structure, phase transformation and prebiotic catalysis in marine manganate minerals. *SIO Ref. Ser.* **81**: 1–19.

Bish, D. L., and E. J. Post. 1989. Thermal behavior of complex, tunnel-structure manganese oxides: *Amer. Mineral.* **74**: 177–186.

Bolton, B. R., R. Both, N. F. Exon, T. F. Hamilton, J. Ostwald, and J. D. Smith. 1988. Geochemistry and mineralogy of seafloor hydrothermal and hydrogenetic Mn oxide deposits from the Manus basin and Bismarck archipelago region of the southwest Pacific ocean. *Mar. Geol.* **85**: 65–87.

Brown, A. C. 1964. Geochemistry of the Dawson settlement bog manganese deposits, New Brunswick. *Geol. Surv. Canada Paper 63-42,* p. 26.

Burns, R. G., V. M. Burns, and H. W. Stockman. 1983. A review of the todorokite-buserite problem: Implication to the mineralogy of marine manganese nodules. *Amer. Mineral.* **68**: 972–980.

Buser, W., P. Graf, and W. Feitknecht. 1954. Beitrag zur Kenntnis der Mangan(II)-manganit und des δ-MnO_2. *Helv. Chim. Acta* **37**: 2322–2333.

Chester, R., and M. J. Hughes. 1976. A chemical technique for the separation of ferro-manganese minerals, carbonate minerals and dsorbed trace elements from pelagic sediments. *Chem. Geol.* **2**: 249–262.

Chukhrov, F. V., A. I. Gorshkov, V. A. Drits, and Y. P. Dikov. 1985. Structural varieties of todorokite. *Int'l Geol. Rev.* **27**: 1481–1491.

Corliss, J. B., M. Lyle, J. Dymond, and K. Crane. 1978. The geochemistry of hydrothermal mounds near the Galapagos rift. *Earth Planet. Sci. Lett.* **40**: 12–24.

Crane, S. E. 1981. Structural chemistry of marine manganate minerals: Ph.D. thesis. Scripps Inst. Oceanography, La Jolla, 296 pp.

Cronan, D. S., G. P. Glasby, S. A. Moorby, J. Thomson, K. E. Knedler, and J. C. McDougall. 1982. A submarine hydrothermal manganese deposit from the S.W. Pacific Island Arc. *Nature* **298**: 456–458.

Dixon, J. B., and H. C. W. Skinner. 1992. Manganese minerals in surface environments. In *Biomineralization Processes of Iron and Manganese—Modern and Ancient Environments.* H. C. W. Skinner and R. W. Fitzpatrick, eds. Cremlingen: CATENA Verlag, 31–50.

Evanson, N. M., P. J. Hamilton, and R. K. O'Nions. 1978. Rare earth abundances in chondritic meteorites. *Geochim. Cosmochim. Acta* **42**: 1199–1212.

Flanagan, F. J., and D. Gotterfried. 1980. USGS Rock Standards, III: Manganese-nodule reference samples USGS-Nod-A-1 and USGS-Nod-P-1. *USGS Prof. Paper 1155,* p. 39.

Giovanoli, R. 1980. On natural and synthetic manganese nodules. In *Geology and Geochemistry of Manganese I.* I. M. Varentsov and G Y. Grasselly, eds. Stuttgart: Schweizerbart'sche Verlag, 159–202.

Giovanoli, R. 1985. Layer structures and tunnel structures in manganates. *Chem. Erde* **44**: 227–244.

Giovanoli, R., and R. Brütsch. 1979. L'echange des ions de transition par le manganate-10Å et le manganate-7Å. In *La Genèse des Nodules de Manganèse.* C. Lalou, ed. Paris: Cent. Natl. Rech. Sci., 305–313.

Glasby, G. P., R. Gwozdz, H. Kunzendorf, G. Friedrich, and T. Thijssen. 1987. The distribution of rare earth and minor elements in manganese nodules and sediments from the equatorial and S.W. Pacific. *Lithos* **20**: 97–113.

Golden, D. C., C. C. Chen, and J. B. Dixon. 1986. Synthesis of Todorokite. *Science* **231**: 717–719.

Govindaraju, K. 1989. 1989 compilation of working values and sample description for 272 geostandards. *Geostandards Newsletter* **13**: 12–13.

Gross, M. G. 1987. *Oceanography—A View of the Earth.* New Jersey: Prentice-Hall Inc., 115–116.

Hariya, Y. 1985. Geochemistry of the hot lake deposits at Oyunuma, Japan, and special reference to recent sulfide deposits around deep-sea vents in the ocean. Proc. 17th OTC, Houston, Texas, 61–65.

Hariya, Y., H. Miura, and N. Mita. 1992. Manganese and manganiferous deposits of the Northern Hokkaido. In *Mineral Deposits of Japan and the Philippines.* 29th Int'l Geol. Congr. Field Trip Guidebook 6. T. Urabe and M. Aoki, eds., 1–16.

Hein, J. R., C. L. Fleishman, L. A. Morgenstein, S. H. Bloomer, and R. J. Stern. 1987. Submarine Ferromanganese deposits from the Mariana and Volcano volcanic arcs, West Pacific. *U.S.G.S. Open File Rept.* **87-281**: 1–9.

Kimura, M., S. Uyeda, Y. Kato, T. Tanaka, M. Yamano, T. Gamo, H. Sakai, S. Kato, E. Izawa, and T. Oomori. 1988. Active hydrothermal mounds in the Okinawa Trough back-arc basin, Japan. *Tectonophysics.* **145**: 319–324.

Klug, H. P., and L. E. Alexander. 1954. *X-ray Diffraction Procedures for Polycrystalline and Amorphous Materials.* New York: John Wiley & Sons, Inc., 491–511.

Krom, M. D., and R. A. Berner. 1983. A rapid method for determination of organic and carbonate carbon in geological samples. *J. Sed. Petrol.* **53**: 600–603.

Kunzendorf, H., G. P. Glasby, P. Stoffer, and W. L. Plüger. 1993. The distribution of rare earth and minor elements in manganese nodules, micronodules and sediments along an east-west transect in the southern Pacific. *Lithos* **30**: 45–56.

Lalou, C., E. Bricht, C. Jehanno, and H. Perez-Leclaire. 1983. Hydrothermal manganese oxide deposits from the Galapagos mounds, DSDP Leg 70, hole 509B and "Alvin" dives 729 and 721. *Earth Planet. Sci. Lett.* **63**: 63–75.

Lonsdale, P., V. M. Burns, and M. Fisk. 1980. Nodules of hydrothermal birnessite in the caldera of a young seamount. *Jour. Geol.* **88**: 611–618.

McKenzie, R. M. 1971. The synthesis of birnessite, cryptomelane, and some other oxides and hydroxides of manganese. *Mineral. Mag.* **28**: 493–503.

Mita, N., A. Maruyama, A. Usui, T. Higashihara, and Y. Hariya. 1994. A growing deposit of hydrous manganese oxide produced by microbial mediation at a hot spring, Japan. *Geochemical Journal* **28**: 71–80.

Mitani, K., T. Fujiwara, and S. Ishiyama. 1964. *Geological Map of Kamiashoro with Explanatory Text* (Kushiro No. 6): Geol. Surv. Hokkaido, 1 sheet [in Japanese].

Miura, H., and Y. Hariya. 1984. Todorokite with long spacing and structure of manganese dioxide minerals. *Jour. Mineral. Soc. Japan* **16**: 301–308 [in Japanese].

Moore, W. S., and P. R. Vogt. 1976. Hydrothermal manganese crusts from two sites near the Galapagos spreading axis. *Earth Planet. Sci. Lett.* **29**: 349–356.

Mustoe, G. E. 1981. Bacterial oxidation of manganese and iron in a modern cold spring. *Geol. Soc. Amer. Bull. Part I* **92**: 147–153.

Paterson, E., J. L. Bunch, and D. R. Clark. 1986a. Cation exchange in synthetic manganates: I. Alkylammounium exchange in a synthetic phyllomanganate. *Clay Miner.* **21**: 949–955.

Paterson, E., D. R. Clark, J. D. Russell, and R. Swaffield. 1986b. Cation exchange in synthetic manganates: II. The structure of an alkylammonium-saturated phyllomanganate. *Clay Miner.* **21**: 957–964.

Post, J. E. 1992. Crystal structures of manganese oxide minerals. In *Biomineralization Processes of Iron and Manganese—Modern and Ancient Environments.* H. C. W. Skinner and R. W. Fitzpatrick, eds. Cremlingen: CATENA Verlag, 51–73.

Post, J. E., and D. L. Bish. 1988. Rietveld refinement of the todorokite structure. *Amer. Miner.* **73**: 861–869.

Potter, R. M., and G. R. Rossman. 1979a. Mineralogy of manganese dendrites and coatings. *Amer. Miner.* **64**: 1219–1226.

Potter, R. M., and G. R. Rossman. 1979b. The tetravalent manganese oxides: identification, hydration, and structural relationships by infrared spectroscopy. *Amer. Miner.* **64**: 1199–1218.

Raymond, Jr., R., G. D. Guthrie, D. L. Bish, S. L. Reneau, and S. J. Chipera. 1992. Biomineralization of manganese in rock varnish. In *Biomineralization Processes of Iron and Manganese—Modern and Ancient Environments.* H. C. W. Skinner and R. W. Fitzpatrick, eds. Cremlingen: CATENA Verlag, 321–335.

Robinson, G. D. 1993. Major-element chemistry and micromorphology of Mn-oxide coatings on stream alluvium. *Appl. Geochem.* **8**: 633–642.

Robbins, E. I., J. P. D'Agostino, J. Ostwald, D. S. Fanning, V. Carter, and R. L. Van Hoven. 1992. Manganese nodules and microbial oxidation of manganese in the Huntley Meadows wetland, Virginia, USA. In *Biomineralization Processes of Iron and Manganese—Modern and Ancient Environments.* H. C. W. Skinner and R. W. Fitzpatrick, eds. Cremlingen: CATENA Verlag, 179–202.

Sato, Y. 1991. Formation of manganese and iron oxides and behavior of associated metal elements: Ph.D. thesis. Tokai University, Shimizu, Japan, 162 pp. [in Japanese].

Satoh, H. 1964. *Geological Map of Akanko with Explanatory Text* (Kushiro No. 7): Geol. Surv. Hokkaido, 1 sheet.

Suzuki, R., and S. Sakai. 1991. Manganese deposits formed from hot-spring waters: *Chikyukagaku (Geochemistry)* **24**: 55–64 [in Japanese].

Takematsu, N., H. Kusakabe, Y. Sato, and S. Okabe. 1988. Todorokite formation in seawater by microbial mediation. *Jour. Oceanogr. Soc. Japan* **44**: 235–242.

Thompson, G., M. J. Mottl, and P. A. Rona. 1985. Morphology, mineralogy and chemistry of hydrothermal deposits from the tag area, 26°N mid-Atlantic ridge. *Chem. Geol.* **49**: 243–257.

Turner, S., M. D. Siegel, and P. R. Buseck. 1982. Structural features of todorokite intergrowths in manganese nodules. *Nature* **296**: 841–842.

Umemoto, S., A. Matsumura, M. Yamaya, and K. Ishibashi. 1956. Report of survey of sulfur, iron and manganese deposits around Mt. Me-Akan. *Data Report of Underground Mineral Resources in Hokkaido* **24**: 21–35 [in Japanese].

Usui, A. 1979. Nickel and copper accumulation as essential elements in 10 Å manganite of deep-sea manganese nodules. *Nature* **279**: 411–413.

Usui, A., and A. Nishimura. 1992. Submersible observation of hydrothermal manganese deposits on the Kaikata Seamount, Izu-Ogasawara (Bonin) Arc. *Mar. Geol.* **106**: 203–216.

Usui, A., T. A. Mellin, M. Nohara, and M. Yuasa. 1989. Structural stability of marine 10Å manganates from the Ogasawara (Bonin) Arc. Implication for low-temperature hydrothermal activity. *Mar. Geol.* **86**: 41–56.

Usui, A., M. Yuasa, M. Yokota, A. Nishimura, and F. Murakami. 1986. Submarine hydrothermal manganese deposits from the Ogasawara (Bonin) Arc, off the Japan Islands. *Mar. Geol.* **73**: 311–322.

Wada, H., A. Seirayasakol, M. Kimura, and Y. Takai. 1978. The process of manganese deposition in paddy soils (I) A

hypothesis and its verification. *Soil Sci. Plant Nutr.* **24**: 55–62.

Yokoyama, I., Y. Katsui, S. Ebara, and K. Koide. 1976. Mt. Me-Akan Dake. Report on volcanoes in Hokkaido, 138 pp. [in Japanese].

Yoshimura, T. 1952. *Manganese Deposits of Japan. I.* Kyushu: Shuko Publ. Co., 567 pp. [in Japanese].

(Received 10 March 1994; accepted 7 July 1994; Ms. 2476)